

# The NATO STO Task Group AVT-201 on 'Extended Assessment of Stability and Control Prediction Methods for NATO Air Vehicles'

Russell M. Cummings\*  
United States Air Force Academy, USAF Academy CO, USA

Andreas Schütte†  
German Aerospace Center (DLR), Braunschweig, Germany

The ability to accurately predict both static and dynamic stability characteristics of air vehicles using computational fluid dynamics (CFD) methods could revolutionize the air vehicle design process, especially for military air vehicles. A validated CFD capability would significantly reduce the number of ground tests required to verify vehicle concepts and, in general, could eliminate costly vehicle 'repair' campaigns required to fix performance anomalies that were not adequately predicted prior to full-scale vehicle development. This paper outlines the extended integrated experimental and numerical approach to assess the of stability and control prediction method capabilities as well as the design and estimation the control device effectiveness for highly swept low observable UCAV configurations. The aim of the AVT-201 Task Group is to provide an assessment of the CFD capabilities using model scale experiments and transferring this knowledge to real scale applications.

## Nomenclature

$\alpha$	=	AoA, Angle of attack [°]	$s$	=	Half span [m]
$\beta$	=	AoS, Angle of side slip [°]	$x$	=	Chord wise coordinate [m]
$\eta$	=	Flap deflection angle [°]	$z$	=	Vertical coordinate [m]
$\Theta$	=	Pitch angle [°]	$y$	=	Span wise coordinate [m]
$\Psi$	=	Yaw angle [°]	$q_\infty$	=	Dynamic pressure coefficient [-] $0.5 \cdot \rho_\infty \cdot V_\infty^2$
$V_\infty$	=	On-flow velocity [m/s]	$C_p$	=	Pressure coefficient [-] $p - p_\infty / q_\infty$
$f$	=	Frequency [Hz]	$C_L$	=	Lift coefficient [-] $L / (q_\infty \cdot A)$
$t$	=	Time [s]	$C_D$	=	Drag coefficient (AE) [-] $D / (q_\infty \cdot A)$
$k$	=	Reduced frequency $2\pi f \cdot c_{ref} / V$	$C_S$	=	Side force coefficient (AE) [-] $S / (q_\infty \cdot A)$
$DoF$	=	Degree of Freedom	$C_m$	=	Pitch moment coefficient (AE) [-] $M / (q_\infty \cdot A \cdot c_{ref})$
$CFRP$	=	Carbon Fiber Reinforced Plastic	$C_l$	=	Roll moment coefficient (AE) [-] $l / (q_\infty \cdot A \cdot s)$
$MRP$	=	Moment Reference Point [m]	$C_n$	=	Yaw moment coefficient (AE) [-] $n / (q_\infty \cdot A \cdot s)$
$AoA$	=	Angle of Attack [°]	$C_z$	=	Normal force coefficient (MF) [-] $F_z / (q_\infty \cdot A)$
$AoS$	=	Angle of Sideslip [°]	$C_y$	=	Side force coefficient (MF) [-] $F_y / (q_\infty \cdot A)$
$SA$	=	Spalart-Allmaras turb. model	$C_{mx}$	=	Roll moment coefficient (MF) [-] $M_x / (q_\infty \cdot A \cdot c_{ref})$
$RSM$	=	Reynolds-Stress turb. model	$C_{my}$	=	Pitch moment coefficient (MF) [-] $M_y / (q_\infty \cdot A \cdot s)$
$A$	=	Reference relation area [m <sup>2</sup> ]	$C_{mz}$	=	Yaw moment coefficient (MF) [-] $M_z / (q_\infty \cdot A \cdot s)$
$c_{ref}$	=	Reference length [m]			
$c_r$	=	Root chord [m]			
$LOB$	=	Left Outboard Trailing Edge Flap	$LE$	=	Leading Edge
$LIB$	=	Left Inboard Trailing Edge Flap	$SLE$	=	Sharp Leading Edge
$RIB$	=	Right Inboard Trailing Edge Flap	$RLE$	=	Round Leading Edge
$ROB$	=	Right Outboard Trailing Edge Flap	$RLE-FT$	=	Round Leading Edge – Fixed Transition
$BL$	=	Base Line (no CS deflection)	$CAWAPI$	=	Cranked Arrow Wing Aerodynamics Project Inter.
$CS$	=	Control Surface	$SACCON$	=	Stability And Control Configuration
$AVT$	=	Applied Vehicle Technology			
$STO$	=	Science and Technology Organization			
$RTO$	=	Research and Technology Organization			

\* Professor of Aeronautics and Head, Department of Aeronautics. AIAA Associate Fellow.

† Research Scientist, Institute of Aerodynamics and Flow Technology. AIAA Senior Member.



## I. Introduction

**S**TABILITY and control (S&C) engineers have used an iterative process combining semi-empirical lower-order, wind-tunnel, and flight test modeling techniques to determine the aerodynamic characteristics of new fighter aircraft. Despite their greatest efforts using the best available predictive capabilities, nearly every major fighter program since 1960 has had costly nonlinear aerodynamic or fluid-structure interaction issues that were not discovered until flight testing.<sup>1-5</sup> Some examples include the F-15,<sup>6</sup> F/A-18,<sup>6</sup> F/A-18C,<sup>7</sup> AV-8B,<sup>6</sup> and the B-2 Bomber.<sup>8</sup> The F-15, F/A-18A, and AV-8B all exhibited significant aero-elastic flutter,<sup>6</sup> while the F/A-18C experienced tail buffet at high angles of attack due to leading-edge extension vortex breakdown,<sup>7</sup> and the B-2 Bomber experienced a residual pitch oscillation.<sup>8</sup> The development costs of each of these aircraft could have been drastically reduced if these issues had been identified earlier in the design process. Clearly, a high-fidelity tool capable of reliably predicting and/or identifying configurations susceptible to handling quality instabilities prior to flight testing would be of great interest to the S&C community. Such a tool would be well suited to the aircraft design phase and would decrease the cost and risks incurred by flight-testing and post-design-phase modifications.

Several tools can be used to predict the S&C characteristics of an aircraft, including flight and wind tunnel testing, semi-empirical lower-order modeling and computational fluid dynamics (CFD). Flight testing is the most accurate of these methods, but is also the most expensive and cannot be used during early stages of the aircraft development process because the aircraft configuration typically is not finalized. Wind tunnel testing is also accurate, but suffers from scaling issues, along with difficulty modeling unsteady dynamic behavior. Wind tunnel testing is also expensive, although cheaper than flight testing. Semi-empirical lower-order modeling has less fidelity than flight and wind-tunnel testing and is incapable of reliably predicting unsteady nonlinear aerodynamic behavior. A reasonable compromise between flight and wind tunnel testing and semi-empirical lower-order modeling is CFD simulation. Modern CFD techniques have a relatively high level of fidelity and have successfully modeled the nonlinear aerodynamic behavior of aircraft at full scale Reynolds numbers. This method reduces some of the major uncertainties associated with sufficiently modeling physical space. However, it comes with an additional cost in execution time that results from computer performance and small physical time step requirements to accurately capture the flow physics. This is exaggerated by the low frequency nature of most of the aerodynamic motions that result in nonlinear behavior of interest. Researchers at NASA Ames, for example, have attempted to perform a "brute force" approach to filling a stability and control database for vehicle design.<sup>9-11</sup> They found that a reasonable database for static stability and control derivatives would include on the order of 30 different angles-of-attack, 20 different Mach numbers, and 5 different side-slip angles, each for a number of different geometry configurations or control surface deflections.<sup>9</sup> They envisioned that a few hundred solutions can be obtained automatically and the remainder of the parameter space is filled using an interpolation procedure or neural networks.

Considering today's performance of computers and CFD codes, the routine calculations of hundreds of maneuvers in a reasonable time frame is unrealistic. In order to accurately and reliably predict the stability and control characteristics of an aircraft prior to the costly flight test phase, CFD has to be combined with predictive modeling of lower complexity. The vision of using CFD in the initial aircraft design phases initiated several projects within S&C, CFD, and wind tunnel communities, including Computational Methods for Stability and Control (COMSAC)<sup>3</sup> and Simulation of Aircraft Stability and Control Characteristics for Use in Conceptual Design (SIMSAC). These groups have met with varying degrees of success, and also helped to formulate the creation of a NATO Research & Technology Organization (RTO) group that would investigate some of these issues.

## II. AVT-201 Task Group

The NATO STO AVT-201 Task Group was established as an extension to the AVT-161 Task Group, which was described in detail in Ref. 12. The purpose of AVT-161 was to determine the ability of computational methods to accurately predict both static and dynamic stability of air and sea vehicles. AVT-201 took on the additional tasks of including control surface deflections in the aerodynamic evaluation, as well as to investigate ways to create full flight simulations using CFD. Whereas this paper will concentrate on the air vehicle application within the Task Group, the overall approach is to identify major synergy in terms of physical modeling, fluid structures, or transition effects.

The topics covered by AVT-201 are to include the following:

- Perform additional in-depth correlation studies
  - Evaluate the ability of CFD to accurately predict S&C for dynamic maneuvers using experimental data obtained by AVT-161
  - Use the detailed flow field measurements (such as PIV data) obtained by AVT-161 to enhance understanding of discrepancies between predicted and experimental dynamic derivatives
  - Further analyze AVT-161 data for cases with flow asymmetry and highly unsteady flow to extend understanding of vehicle dynamics (air activity)

- Perform additional wind and/or water tunnel/channel testing to extend the dynamic data set to include multiple frequency and amplitude maneuvers to improve the determination of realistic dynamic derivatives
- Obtain, where possible, full-scale test data for a maneuvering vehicle that can be used for validation of the methods and capabilities that are developed
- Investigate control surface effects on dynamic S&C
  - Design, build, and test modified SACCON wind tunnel model with trailing-edge control surfaces (static deflections)
  - Evaluate ability to predict control effectiveness, stability characteristics, and other flight mechanic characteristics of the configuration with controls deflected
- Investigate techniques for creating flight simulation models from CFD predictions
  - Build S&C data bases from experimental and CFD predictions to compare impact on flight simulation accuracy
  - Determine level of accuracy and sensitivity of flight simulation using CFD when compared with experimental data model
  - Explore range of strategies for creating CFD-derived simulation models across the flight envelope (such as reduced-order modeling or combined low-fidelity/high-fidelity approaches)
- International collaboration
  - The concept of a virtual laboratory, as pioneered by AVT-113, and used to great effect in AVT-161, will be employed by the new Task Group in order to make the data being measured and computed available to the participants on a timely basis

The AVT-201 Task Group partners and their contributions are listed in **Table 1**. There are 16 different organizations making contributions from 5 different NATO nations, as well as Sweden and Australia. A wide variety of contributions are included, such as wind tunnel model development, wind tunnel testing, CFD predictions, engineering method analysis, and development of stability and control (S&C) models of various types. This represents a wide variety of participation that makes the AVT-201 (and its predecessor AVT-161) very prolific and successful task groups.

Organisation	Contribution				
	SACCON configuration+model	Experiment	CFD	Engineering Methods	S&C
NASA	x		x		x
DLR	x	x	x	x	
USAF			x		x
DNW-NWB		x			
Airbus D&S			x		
BAE Systems		x	x		x
DSTL		x	x		
DSTO			x		
FOI			x		
KTH			x	x	
NLR			x		
Nangia ARA				x	
NavAir			x		
ONERA		x	x		x
Univ. of Liverpool			x		
TU Braunschweig	Vortical flow consultant				

**Table 1:** AVT-201 Task Group participants and contributions.



### III. Configuration and Wind Tunnel Models

While AVT-161 Task Group conducted wind tunnel tests of two highly swept wing configurations (the X-31 and SACCON), AVT-201 has primarily concentrated on SACCON. The planform and section profiles were defined in cooperation between DLR and EADS-MAS during the early stages of AVT-161. DLR adjusted the pre-design geometry for wind tunnel design purposes which actually led to a higher overall thickness at the root chord to provide enough space for the internal strain gauge balance. The SACCON UCAV has a lambda wing plan form with a leading edge sweep angle of  $53^\circ$  (see Figures 1 and 2). The root chord is approximately 1m and the wing span is 1.53 m. The main sections of the model are the fuselage, the wing section and wing tip. The configuration is defined by three different profiles at the root section of the fuselage, two sections with the same profile at the inner wing, forming the transition from the fuselage to wing and the outer wing section. Due to radar signature issues the leading edge is parallel to the wing trailing edges and the wing tip is designed parallel to the trailing edge of the fuselage section. Finally the outer wing section profile is twisted by  $5^\circ$  around the leading edge to reduce the aerodynamic loads and shifting the onset of flow separation to higher angles of attack.

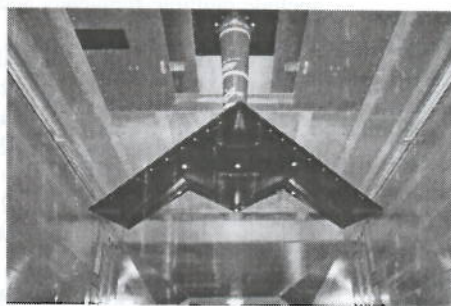


**Figure 1:** UCAV low speed wind tunnel model SACCON on the MPM-“Model Positioning Mechanism” in the closed test section of the Low Speed Wind Tunnel Braunschweig (DNW-NWB).

Four wind tunnel model configurations have been used to conduct experimental data within the AVT-201 Task Group. All wind tunnel models based on the SACCON geometry developed within the predecessor Task Group AVT-161 where the focus has been to investigate the aerodynamic stability and control behavior and the detailed flow physics of the clean configuration.<sup>13,14</sup> In the present Task Group the configurations have been extended by establishing trailing edge control devices.<sup>15</sup> Furthermore, a third model has been established for the high speed regime to establish a more comprehensive experimental data set to cover wider Mach number range. Finally, ONERA has constructed a wind tunnel model for their rotary rig wind tunnel tests.

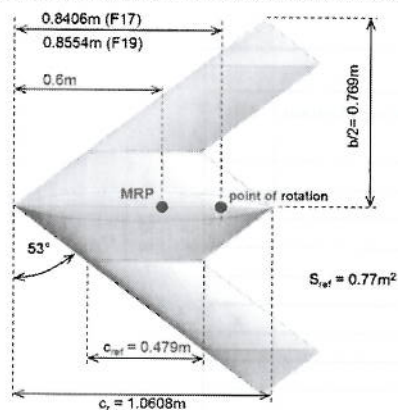


**Figure 2:** Planform and geometric parameters of the generic UCAV configuration (Models F-17 and F-19).

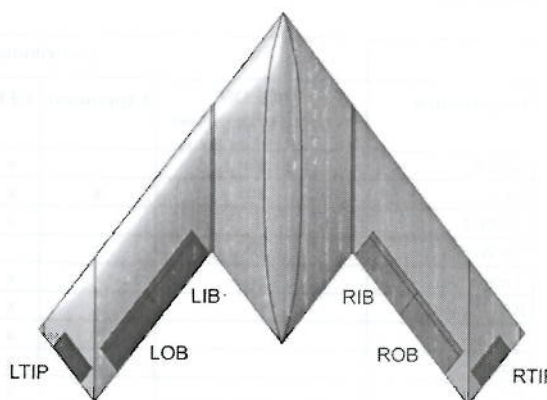


**Figure 3:** Control surface layout and designation; L=Left, R=Right. IB=Inboard, OB=Outboard.

Fig. 1 shows the original SACCON wind tunnel model in the DNW-NWB wind tunnel. The model used within the AVT-161 Task Group was first extended by adding control devices to the left hand side of the trailing edge. The control devices were exchanged to investigate different control device setups. Figure 2 shows the DLR F-17 and DLR F-19 model configurations based on the same geometry as the SACCON model but with trailing edge control devices on both sides of the wing, as shown in Figure 3. Both wind tunnel models are designed for low speed flow conditions. Figure 4 shows the DLR F-17E wind tunnel model configuration designed for medium to high speed flow conditions up to the transonic regime. The clean wing geometry of the DLR F-17E model is also based on the SACCON geometry and the trailing edges can be extended with control devices. The setup of the trailing edge control devices is exchangeable in the same manner as for the two low speed model configurations.<sup>14</sup> Finally, the ONERA SACCON low speed configuration, which is also based on the SACCON geometry, had a root chord of 0.311m and a semi-span of 0.5m. The ONERA model has no control devices but was used within the Task Group to extend the dynamic experimental data set.

Several wind tunnel investigations have been established from low speed up to transonic Mach number regime using all four wind tunnel models. Static and dynamic wind tunnel tests have been conducted with the SACCON



and the DLR F-19 wind tunnel model by NASA and DLR in the low speed wind tunnel facility of the DNW at the DLR venue in Braunschweig, Germany. Within several test campaigns the static aerodynamics and stability and control behavior has been assessed for different control device setups in comparison to the base line configuration without trailing edge control devices. Furthermore, dynamic maneuver simulations have been investigated to assess the aerodynamic dynamic stability and control behavior. Additional static and dynamic low speed wind tunnel tests have been established on the rotary balance in the SV4A and the L1 wind tunnel facilities at ONERA in Lille, France.

The medium to high speed wind tunnel tests have been conducted at DLR in the Transonic Wind Tunnel Göttingen (DNW-TWG) in Germany and at the high speed wind tunnel facility (HSWT) of BAE Systems at the Warton Aerodrome in the United Kingdom. The latter was a common test campaign by BAE Systems, DSTL, and DLR. Both wind tunnel entries have been designed in an integrated fashion in order to cover the entire Mach number range and a maximum of possible control device deflection combinations within the given test campaign time frame.

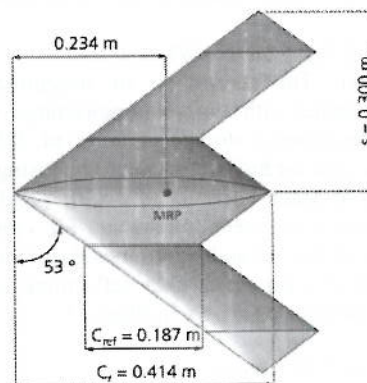


**Figure 4:** Planform and geometric parameters of the generic UCAV configuration (F-17E).

## IV. Experimental Approach

The following section describes the wind tunnel facilities used for establishing the steady state and dynamic experimental data for the SACCON configurations with control surfaces.

### A. Experimental Facilities

Four wind tunnel model configurations have been used to conduct experimental data within the AVT-201 Task Group. All wind tunnel models are based on the SACCON geometry developed within the predecessor Task Group AVT-161 where the focus was to investigate the aerodynamic stability and control behavior and the detailed flow physics of the clean configuration.<sup>13,14</sup> In the present Task Group the configurations have been extended by establishing trailing edge control devices.<sup>15</sup> Furthermore, a third model has been established for the high speed regime to establish a more comprehensive experimental data set to cover wider Mach number range.

#### 1. Low Speed Wind Tunnel Braunschweig (DNW-NWB)

The DNW-NWB belongs to the foundation “German–Dutch Wind Tunnels” under Dutch law. DNW operates 12 different wind tunnels on five sites in Germany and the Netherlands. The DNW-NWB is located on the DLR site in Braunschweig, Germany. It is a closed-circuit, atmospheric type wind tunnel, which can be operated either with an open, slotted or closed test section. The SACCON configuration in the DNW-NWB tunnel with controls surfaces on the left side is shown in Figure 5; the DLR F-19 configuration with control surfaces on both sides is shown in Figure 6. The test section size is 3.25m by 2.8m (10.6ft by 9.2ft). The maximum free stream velocity is  $V = 80$  m/s (263 ft/s) in the closed test section and  $V = 70$  m/s (230 ft/s) in the open test section. NWB’s model supports include basic  $\alpha$ - $\beta$ -support, half-model support, support for 2D models, a rotary motion support for rolling and spinning tests and the Model Positioning Mechanism (MPM), which was described in Ref. 12.

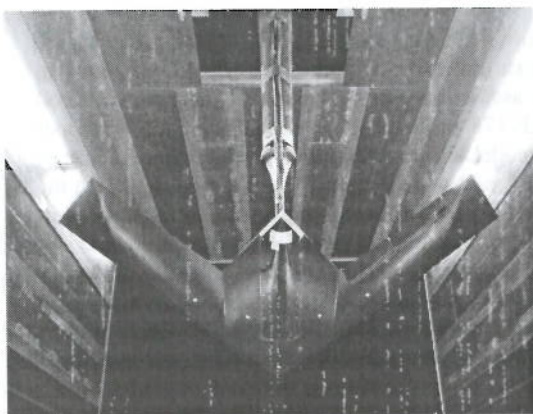


**Figure 5:** SACCON wind tunnel model with control surfaces on the left hand side of the trailing edge in the DNW-NWB, mounted on the MPM support.

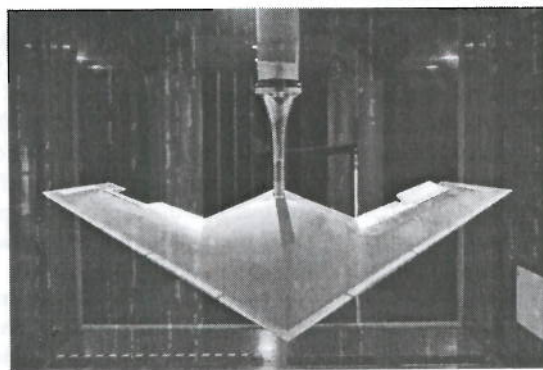


**Figure 6:** DLR F-19 wind tunnel model with control surfaces at the TE on both sides of the configuration in the DNW-NWB, mounted on the MPM support.



## 2. BAE Systems High Speed Wind Tunnel (HWST)

The BAE Systems HWST is a 1.2m by 1.2m Trisonic wind tunnel. The tunnel is an intermittent Trisonic blowdown tunnel with a Mach number range of 0.4 to 3.7 that operates from a storage pressure of 4200 kPa. The tunnel was used for high subsonic testing using the DLR F-17E model at Mach numbers of 0.5, 0.7, and 0.85. Force and moment tests were conducted for control surface deflections of the left and right inboard and outboard flaps were tested at a variety of flap deflections and angles of attack and sideslip, as shown in Figure 7.

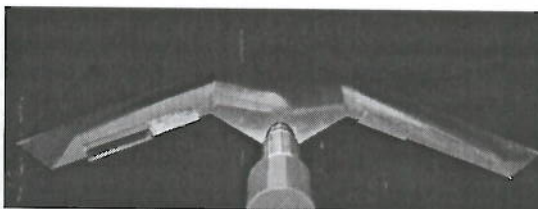


Figure 7: DLR F-17E wind tunnel model with control surfaces at the BAE Systems HWST.

## 3. ONERA L1/SV4 Wind Tunnels

The ONERA L1 wind tunnel is an Eiffel type wind tunnel with a return hall and installed power of 650 kW. The tunnel can be operated at variable speeds up to 75 m/s with a 2.40m diameter test section. A new SACCON model was built for these tests with a variety of control surfaces to take advantage of the PQR rotary rig in the open jet test section, as shown in Figure 8.

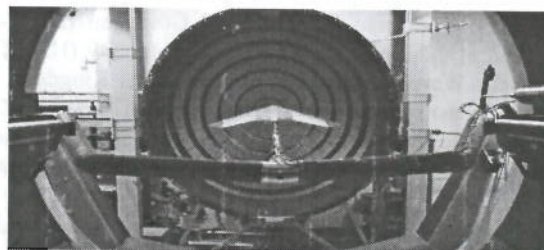


Figure 8: ONERA SACCON wind tunnel model in the ONERA L1 wind tunnel facility on the PQR Rig.

The ONERA SV4 wind tunnel is a vertical, low speed, Eiffel type wind tunnel with a streamline return corridor. The open test section has a 4m diameter with a length of 4m. The rotary balance is an apparatus that allows the following tests:

- Static tests where the angle of attack is varying between  $0^\circ$  and  $30^\circ$  at given sideslip angle and angle of sideslip is varying between  $0^\circ$  and  $30^\circ$  (or  $-30^\circ$ ) at given angle of attack
- Coning tests (rotation about wind axis at constant AoA and AoS). The rotation rate can vary continuously during a test between  $-600^\circ/\text{s}$  and  $+600^\circ/\text{s}$  which allows for identifying non-linearities with respect to frequency

The oscillatory coning tests differ from the previous tests in the fact that the  $\lambda$  angle (the angle between the axis of rotation and the free stream axis) is set to a non-zero value, which induces periodic variations of the angle of attack and the sideslip angles during one turn. The amplitude of those variations is equal to  $\lambda$ . For purpose of identification of dynamic derivatives the rotation rates are generally set to  $30^\circ/\text{s}$ ,  $\pm 600^\circ/\text{s}$  and value of the  $\lambda$  angle is generally chosen equal to  $5^\circ$  in order to not obtain large variations of angles of attack and sideslip and therefore not to induce non-linear effects.

## 4. Transonic Wind Tunnel Göttingen (DNW-TWG)

The Transonic Wind Tunnel in Göttingen (TWG) is a facility for research and development tests in the transonic domain. The closed circuit, continuous, sub-, trans- and supersonic wind tunnel has three exchangeable test sections with a 1m by 1m cross section. The tunnel is able to operate at Mach numbers from 0.3 to 2.2. The DNW-TWG also belongs to the foundation "German-Dutch Wind Tunnels," the same as the DNW-NWB.

### B. Measurement techniques

The wind tunnel models for the low and high speed test regimes were applied with transition tripping to assure fully turbulent flow conditions. For the SACCON and DLR F-19, a strip of carborundum grit was applied according to procedures established in the test campaigns for AVT-161. To assure fully turbulent flow conditions, infrared measurements have been done and reported in Ref. 12. The DLR F-17E model utilized tripping dots on the upper and lower side of the wing around the leading edge. The ONERA model also used trip dots on the upper surface of the leading edge. For CFD prediction purposes fully turbulent flow conditions are much easier to simulate with the present CFD methods and not all partner had the capability to predict a free transition in their computational codes. Furthermore, the knowledge of the flow conditions is of paramount importance for these tests since the results are used for CFD validation.

In all wind tunnel tests forces and moments have been measured with internal six component strain gauge balances. The low speed wind tunnel models are equipped with pressure sensors on the upper and lower surface of the wing at certain  $x$  = constant locations on the front part and normal to the wing leading edge at the rear portion of the wing. For the DLR F-17E model pressure sensitive paint was applied to provide the pressure distribution on the upper side of the wing.



Both low speed wind tunnel models have been mounted on a belly sting at the lower end of the configuration. The sting was mounted on the DNW-NWB MPM system (Model Positioning Mechanism) which allows maneuver simulation in the wind tunnel.<sup>14,15</sup> For the high speed test the DLR F-17E model was mounted on a rear sting support in the TWG and HSWT wind tunnel facilities. The ONERA SACCON model has been mounted in both ONERA wind tunnel facilities on a rear sting support as well. On the rotary balance the model was used to conduct dynamic rotating motions around the wind axis. In the ONERA L1 wind tunnel facility static and dynamic roll, pitch and yaw motions have been conducted.

### C. Wind tunnel tests

The various wind tunnel models described above have been used in numerous wind tunnel tests to determine the aerodynamic characteristics of the SACCON configuration. The tests included low speed tests with control surface

Model	Mach Number	Reynolds number	Test Section	Support	Facility
SACCON	0.145	$1.56 \cdot 10^6$	closed	belly sting	DNW-NWB
DLR F-19	0.145	$1.56 \cdot 10^6$	closed	belly sting	DNW-NWB
DLR F-17E	0.3 0.4 0.5 0.6 0.7	$0.84 \cdot 10^6$	closed	aft sting	DNW-TWG
	0.4	$0.55 \cdot 10^6$ $1.10 \cdot 10^6$ $1.46 \cdot 10^6$ $1.84 \cdot 10^6$	closed	aft sting	DNW-TWG
	0.75	$2.45 \cdot 10^6$	closed	aft sting	DNW-TWG
	0.5 0.7 0.8 0.85 0.9	$3.4 \cdot 10^6$ $4.3 \cdot 10^6$ $4.5 \cdot 10^6$ $4.8 \cdot 10^6$ $4.9 \cdot 10^6$	closed	aft sting	HSWT
	0.5 0.7 0.8 0.85 0.9	$2.1 \cdot 10^6$ $2.6 \cdot 10^6$ $2.8 \cdot 10^6$ $2.85 \cdot 10^6$ $3.0 \cdot 10^6$	closed	aft sting	DNW-TWG
	0.1 0.13	$0.96 \cdot 10^6$ $0.74 \cdot 10^6$	open	aft sting	ONERA SV4 and L1
ONERA SACCON	0.1 0.13	$0.96 \cdot 10^6$ $0.74 \cdot 10^6$	open	aft sting	ONERA SV4 and L1

**Table 2:** Matrix of wind tunnel test campaigns and test conditions for AVT-210.

deflections, low speed tests with dynamic motion, and high subsonic speed tests with control surface deflections (see Table 2). In addition, rotary rig tests were conducted at ONERA. The Mach number range of the resulting tests creates an impressive span of the subsonic regime, including overlap at Mach 0.5 and 0.7. Since all of the models had boundary layer trips, the Reynolds number differences probably play a minimal role in the results.

## V. Experimental Results

The experimental results from all wind tunnel tests were first used to validate the computational simulations and to analyze the flow physics. The focus on comparisons is on the differences between the baseline configuration and

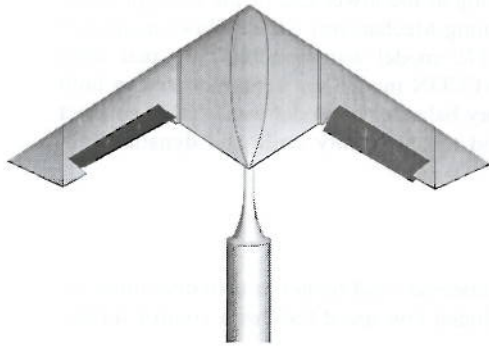


**Figure 9:** F-19 model with 20 degrees of aileron deflections;  $\eta = -20^\circ$  deflected TE control devices on the left hand side and  $\eta = 20^\circ$  on the right hand side.

the configuration with control device deflections. The main objectives are to set up an aerodynamic model for stability and control analyses of the present UCAV configuration. This will be done by a system identification process of the entire experimental data set. After the S&C behavior is modeled, it will be assessed by use of the aerodynamic model and compared with analysis using CFD simulation results substituting the experimental data (or portions of it). The purpose is to evaluate the current status of the CFD prediction capabilities of the S&C behavior of configurations with non-linear aerodynamics.

An example of the wind tunnel results can be seen in Figs. 9 and 10, where aerodynamic coefficients for two wind tunnel runs are compared (specifically, lift, pitch moment, roll moment, and yaw moment coefficients are presented). The control surface run represents 20 degrees of aileron using all four control surfaces, as shown in Fig. 9. In this case the baseline results (BL) are shown with open symbols colored by the particular aerodynamic coefficient (Fig. 10). For example, the pitch moment coefficient is shown with the open blue symbols and demonstrates the non-linear behavior of the vehicle at angles of attack above approximately 10 degree angle of attack. Notice the impact of the aileron deflection on the roll moment (green symbols) with the corresponding cross-coupling for the yaw moment (magenta symbols). As expected, the impact on the longitudinal coefficients (lift and pitch moment) are relatively small, although the pitch moment slope at lower angles of attack does change noticeably.

Figure 11 shows an example for one of the dynamic motion experiments obtained with the DLR F-19 wind tunnel model mounted on the MPM support in the DNW-NWB. With the MPM and an additional motion link inside the model, multi-frequency, multi-amplitude motions can be simulated. With this generic motion a wide range of frequencies and amplitudes can be measured within one wind tunnel run in comparison to a single event pitching motion. Several of these experiments have been done to provide the dynamic derivatives for the aerodynamic S&C model. In this case, the multi-frequency, multi-amplitude run shows the large impact of the motion on the pitch and roll moment coefficients, which gives the CFD simulations a challenge for matching results and being able to predict non-linear, unsteady

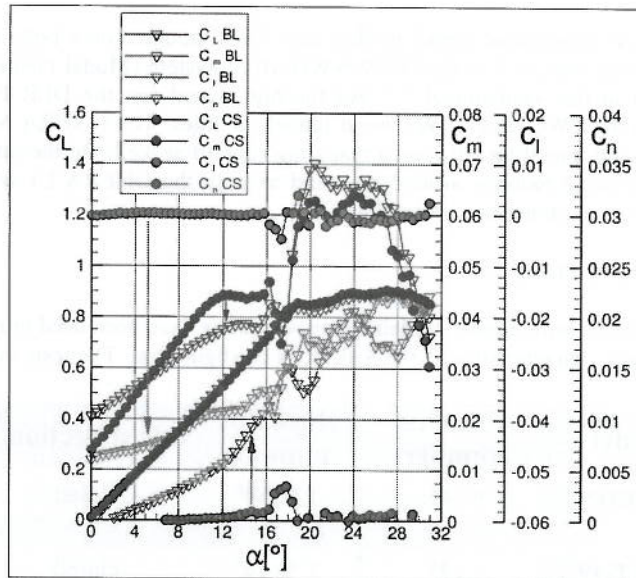


**Figure 10:** Low speed wind tunnel results for the F-19 configuration showing the impact of 20 degrees of aileron control surface deflections: BL = baseline, CS = control surface.

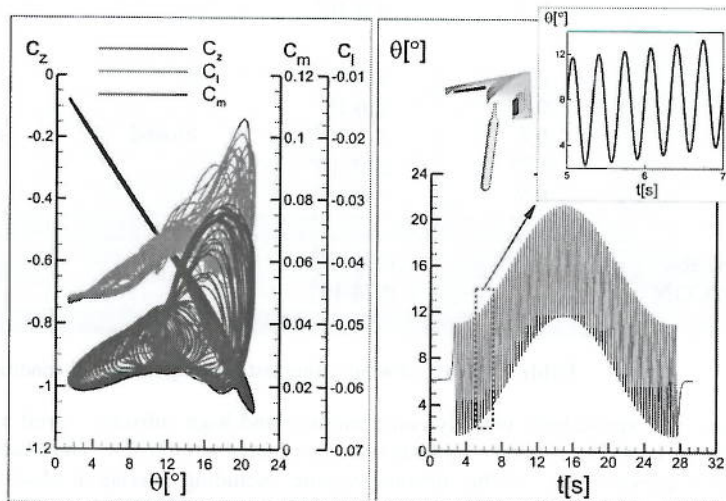


**Figure 11:** Left: Normal force, Pitch and roll moment plotted versus the pitch angle,  $\theta$ . Right: Multi frequency, multi amplitude motion of the DLR F-19 configuration with  $\eta = -20^\circ$  deflected TE control devices on the left hand side and  $\eta = 20^\circ$  on the right hand side.



aerodynamics. Typically, a motion run such as this would result in translating ellipses for a vehicle with linear aerodynamics, but the unusual shapes of the oscillations shows the degree of non-linearity in the results, making the F-19 aerodynamics difficult to simulate.

## VI. Numerical Results

The numerical simulations are being conducted by several partners using various kinds of semi-empirical and Navier-Stokes computational codes using cell-centered or cell-vertex unstructured, block structured, or hybrid grid approaches (see Table 1). Various RANS turbulence models are being employed, as well as hybrid RANS/LES models such as DES and DDES. In addition, several contributions are being made using engineering methods rather than CFD solvers for comparisons in areas of linear aerodynamic behavior. Furthermore different “best practices” experiences exist for each computational method which leads to the necessity to define common procedures or courses of action to be able to compare the different approaches and being able to detect similarities and differences. Guidelines need to be defined, similarities and differences between various approaches have to be detected to develop advanced “best practice” procedures or to identify possible improvements of particular “best practice” procedures. For example, numerical simulations of the flow over the F-19 configuration at  $\alpha = 15^\circ$  and  $\beta = 0^\circ$  are shown in Fig. 12. These comparisons are made using the DLR TAU code and show the complex vortical flow over the configuration (multiple interacting vortices and a tip-stall region). Notice how the flow field changes when the control devices are extended (in this case an aileron deployment of 20 degrees), with the vertical structures changing dramatically, not only in the region of the control surfaces but also near the leading edge where the vortex formation and convection is altered by control surface deflection.

Wind Tunnel Run	LOB	LIB	RIB	ROB	$\alpha$	$\beta$
RN1001	0	0	0	0	10, 15	0
RN1092	0	-20	+20	0	15	0
RN1114	-20	0	0	+20	10, 15	0
RN1103	-20	-20	+20	+20	10, 15	0
RN1007	0	0	0	0	10	10
RN1008	0	0	0	0	14	3
RN1109	-20	-20	+20	+20	10	10
RN1110	-20	-20	+20	+20	14	3

Table 3: Common static test cases

For AVT-201 we defined common test cases based on pre-design CFD calculations which detected the AoA range of interest. Then the participants confirmed to perform CFD simulations using different turbulence models for both static and dynamic cases. A summary of these results may be seen in Ref. 16. For example, the common static test cases are shown in Table 3 (see Fig. 3 for control surface definitions). Cases were chosen to highlight the more challenging flight conditions with and without control surface deflections, especially in the non-linear aerodynamic region that takes place between  $15^\circ$  and  $20^\circ$  angle of attack. Another set of test cases for dynamic motion was also chosen, including cases with pitch oscillations and yaw oscillations.

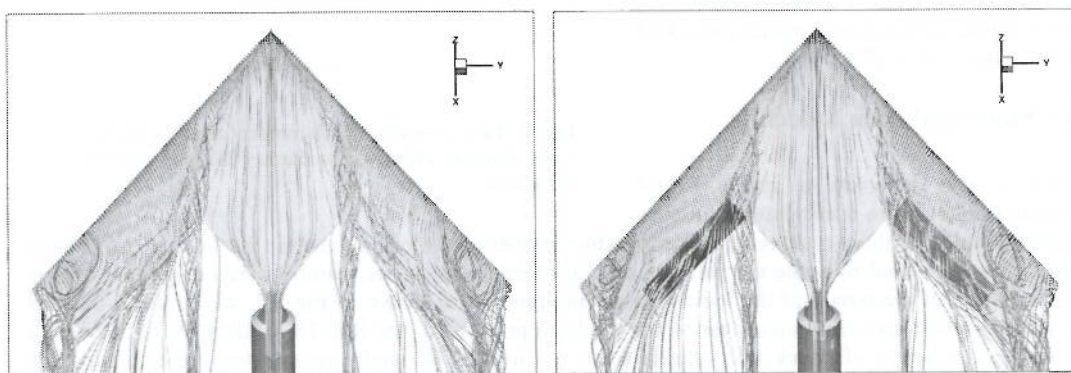
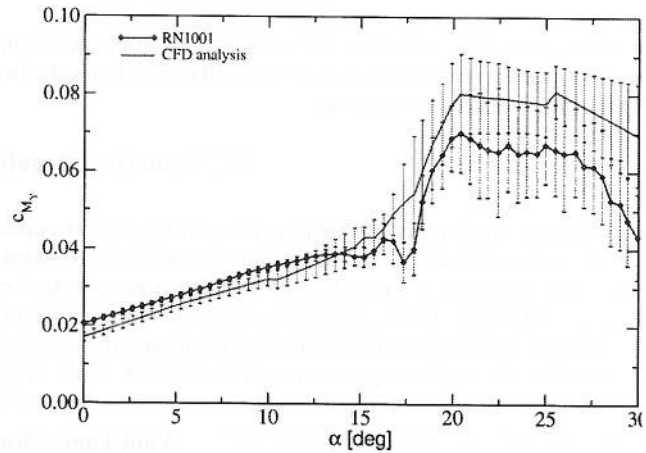


Figure 12: Flow field over clean F-19 configuration, including the sting, at  $\alpha = 15^\circ$  and  $\beta = 0^\circ$ . Right: Flow over F-19 configuration at same flight condition with  $\eta = -20^\circ$  deflected TE control devices on the left hand side and  $\eta = 20^\circ$  on the right hand side.

An example of the results for one static test case, RN1001, is shown in Fig. 13. This case has no control surface deflections, but the experimental results in Fig. 10 show that significant non-linearities for the pitch moment



coefficient exist above 15 degrees angle of attack (pitch moment coefficient results are shown with blue symbols). In Fig. 13 the experimental data is shown in black with bars indicating the unsteadiness range from the wind tunnel tests. Notice that the non-linear region is also the region where the unsteadiness starts to grow dramatically (around 12 degree angle of attack), with significant unsteadiness taking place above 18 degrees. CFD predictions were collected from a number of the participants in AVT-201 using a variety of turbulence models. An average value for their predictions is shown in red in Fig. 13, with the bars indicating a standard deviation range from the average. Notice that the predictions were primarily made with a sting included, however most predictions were made as first-order temporal predictions. Given the highly unsteady flow fields observed by the experiments, unsteady calculations are probably in order for the highest angles of attack. Also notice that the average prediction at 17 degrees AoA does not show the non-linear nature of the pitch moment, although many of the individual predictions do show the non-linearity. While there is still a great deal to learn about the flow field for the higher angles of attack, the predictions are now showing reasonable agreement with the wind tunnel data and will provide an good basis for stability and control estimates.



**Figure 13:** Pitch moment coefficient comparison: experimental data with unsteadiness bars compared with average CFD prediction from all participants with bars indicating one standard deviation; clean F-19 configuration.

## VII. Experimental Data Modeling

Significant effort has also been made to model the experimental aerodynamic data for creation of a 6 DoF simulation of the SACCON vehicle. Both static and dynamic experimental data was collected, various stability derivatives were estimated, and a full aerodynamic model has been created. An example of the process involved is shown in Fig. 14, where the incremental pitch moment coefficient is shown for the SACCON configuration due to left inboard elevon deflections at low speeds. From this information a model of stability derivatives can be created, and when coupled with similar models for other derivatives, a complete model of the aerodynamic characteristics of SACCON can be created. Details of the full modeling process and the resulting aerodynamic model and 6 DoF capability can be found in Ref. 17.

## VIII. Numerical Data Modeling

A parallel effort is also underway to create 6 DoF aerodynamic models solely from numerical predictions.

In order to create the model without making an unmanageable number of static and dynamic predictions, an indicial function approach has been used by some members of the Task Group, and other members are using table lookup approaches. An example of the power of the indicial function approach is shown in Fig. 15, where the SACCON configuration is flying a half lazy eight maneuver which has been prescribed (see Ref. 18 for details). In this case a series of step changes in angle of attack and sideslip were run using CFD and a model was created using the response to the step changes. The model is then used to predict the aerodynamics of the maneuver and is then compared with the full CFD simulation of the maneuver (in this case with no control surface deflections). The comparison shows that the model does a very good job in predicting the aerodynamics of SACCON. Future work will include control surface deflections in the creation of the model.

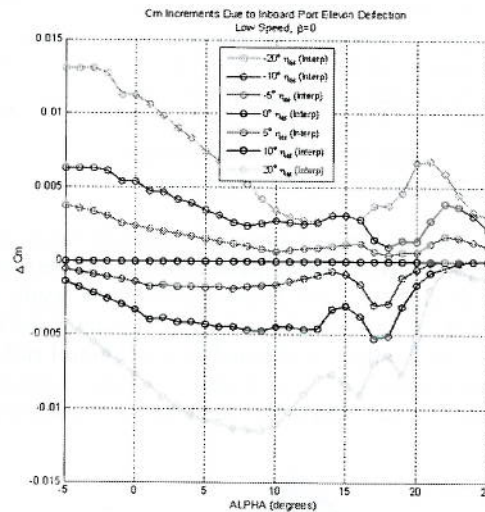


**Figure 14:** Incremental pitch moment coefficient showing control surface effectiveness due to left inboard elevon deflection.



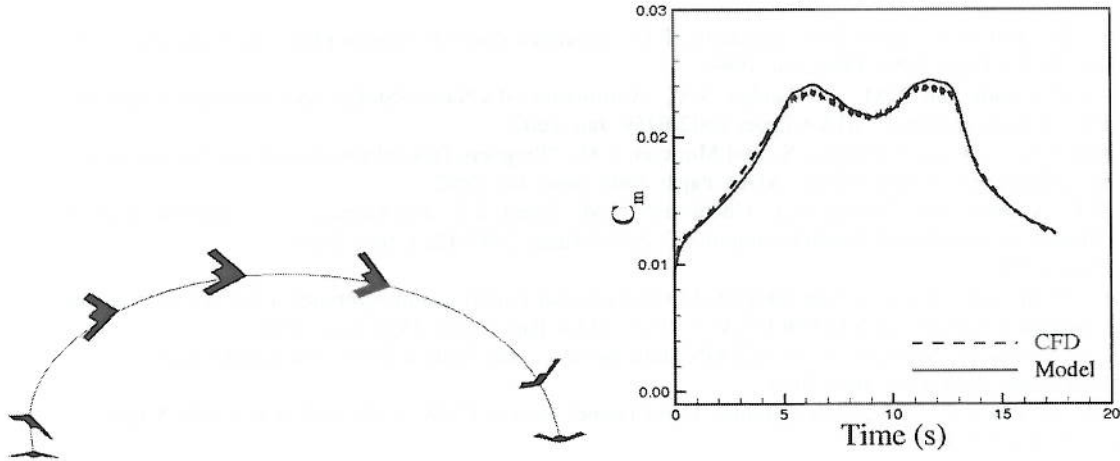


Figure 15: SACCON in a half lazy eight maneuver predicted using indicial functions.

## IX. Conclusions

A NATO STO Task Group, AVT-201, is utilizing state-of-the-art computational and experimental tools to determine the ability to accurately predict the static and dynamic aerodynamics of maneuvering aircraft for stability and control purposes. This is being accomplished by investigating the static and dynamic aerodynamics of SACCON, a generic UCAV. While our overall goal is to determine the state-of-the-art for computational capabilities in predicting stability and control parameters for aircraft, we are also conducting detailed “experiments” to assess the ability of grids, turbulence models, and time integration approaches to accurately predict these complex unsteady flow fields. The end products of this work should greatly increase our understanding of both aerodynamics and our ability to predict complex flow fields with various approaches.

Significant progress has also been made in our predictions of static and dynamic stability parameters for SACCON, as well as our ability to create aerodynamic models for the configuration, and a determination will be made about how well those predictions match the experimental data and the needs of S&C engineers. Those results show that it is possible to create a S&C data base without excessive costs, depending on the accuracy requirements for the model. AVT-201 will continue to make these assessments and improve the prediction of stability and control characteristics of configurations with complex flow fields.

## Acknowledgments

The authors would like to thank DLR, DSTL, BAE Systems, and ONERA for providing wind tunnel test time for the SACCON (and related) configuration(s). Finally, we would like to thank all of the highly motivated participants of the AVT-201 Task Group for their significant contributions.

## References

- <sup>1</sup> Chambers, J.R. and Hall, R.M., “Historical Review of Uncommanded Lateral-Directional Motions at Transonic Conditions,” *Journal of Aircraft*, Vol. 41, No. 3, 2004, pp. 436-447.
- <sup>2</sup> Hall, R.M., Woodson, S.H., and Chambers, J.R., “Accomplishments of the Abrupt-Wing-Stall Program,” *Journal of Aircraft*, Vol. 42, No. 3, 2005, pp. 653-660.
- <sup>3</sup> Hall, R.M., Biedron, R.T., Ball, D.N., Bogue, D.R., Chung, J., Green, B.E., and Chambers, J.R., “Computational Methods for Stability and Control (COMSAC): The Time Has Come,” AIAA Paper 2005-6121, Aug. 2005.
- <sup>4</sup> McDaniel, D.R., Cummings, R.M., Bergeron, K., Morton, S.M., and Dean, J.P., “Comparisons of CFD Solutions of Static and Maneuvering Fighter Aircraft with Flight Test Data,” 3rd International Symposium on Integrating CFD and Experiments in Aerodynamics, 20-21 June 2007, US Air Force Academy, CO.
- <sup>5</sup> Lovell, D. A., “Military Vortices,” NATO RTO/AVT Symposium on Advanced Flow Management, NATO RTO-MP-069, Paper KN-1, March 2003.
- <sup>6</sup> Yurkovich, R., “Status of Unsteady Aerodynamic Prediction for Flutter of High-Performance Aircraft,” *Journal of Aircraft*, Vol. 40, No. 5, 2003, pp. 832-842.



- <sup>7</sup> Meyn, L. A. and James, K. D., "Full Scale Wind Tunnel Studies of F/A-18 Tail Buffet," *Journal of Aircraft*, Vol. 33, No. 3, 1996, pp. 589-595.
- <sup>8</sup> Jacobson, S.B., Britt, R.T., Freim, D.R., and Kelly, P.D., "Residual Pitch Oscillation Flight Test Analysis on the B-2 Bomber," AIAA Paper 1998-1805, Jan. 1998.
- <sup>9</sup> Murman, S.M., Chaderjian, N.M., and Pandya, S.A., "Automation of a Navier-Stokes S&C database generation for the Harrier in Ground Effect," AIAA Paper 2002-0259, Jan. 2002.
- <sup>10</sup> Chaderjian, N.M., Ahmad, J., Pandya, S., and Murman, S.M., "Progress Toward Generation of a Navier-Stokes Database for a Harrier in Ground Effect," AIAA Paper 2002-5966, Jan. 2002.
- <sup>11</sup> Rogers, S.E., Aftomis, M.J., Pandya, S.A., Chaderjian, N.M., Tejnil, E.T., and Ahmad, J.U., "Automated CFD Parameter Studies on Distributed Parallel Computers," AIAA Paper 2003-4229, June 2003. 010-4691, June 2010.
- <sup>12</sup> Cummings, R.M. and Schütte, A. "An Integrated Computational/Experimental Approach to UCAV Stability & Control Estimation: Overview of NATO RTO AVT-161," AIAA Paper 2010-4392, June 2010.
- <sup>13</sup> Löser, T.A., Vicroy, D., Schuette, A., "SACCON Static Wind Tunnel Tests at DNW-NWB and 14'x22' NASA LaRC," AIAA Paper 2010-4393, June 2010.
- <sup>14</sup> Vicroy, D., and Löser, T., "SACCON Dynamic Wind Tunnel Tests at DNW-NWB and 14'x22' NASA LaRC," AIAA Paper 2010-4394, June 2010.
- <sup>15</sup> Huber, K., Vicroy, D.D., Schütte, A., Hübner, A.-R., "UCAV Model Design Investigations and Static Low Speed Wind Tunnel Experiments to Estimate Control Device Effectiveness and S&C Capabilities," 32<sup>nd</sup> AIAA Applied Aerodynamics Conference, Atlanta, GA, 16-20 June, 2014 (submitted for publication).
- <sup>16</sup> Jirásek, A., Cummings, R.M., Schütte, A., and Huber, K., "The NATO STO AVT-201 Task Group on Extended Assessment of Stability and Control Prediction Methods for NATO Air Vehicles: Summary," AIAA Paper 2014-2394, June 2014.
- <sup>17</sup> Irving, J.P., Vicroy, D.D., Farcy, D., and Rizzi, A., "Development of an Aerodynamic Simulation Model of a Generic Configuration for S&C Analyses," AIAA Paper 2014-2393, June 2014.
- <sup>18</sup> Ghoreyshi, M., Jirásek, A., Cummings, R.M., DaRonch, A., and Young, M.A., "Validation of Unsteady Aerodynamic Models of a Generic UCAV Using Overset Grids," AIAA Paper 2014-2265, June 2014.